

# Ionospheric Disturbances at Dawn, Dusk, and During the 2017 Eclipse

*The author reports on ionospheric propagation phenomena during an eclipse and during an ARRL Frequency Measurement Test.*

The author recently participated in the HamSCI propagation experiments during the August 2017 total solar eclipse, and the ARRL November 2017 Frequency Measuring Test (FMT). This article presents some interesting propagation phenomena observed during both activities. For the eclipse experiment, well-defined propagation enhancements of both 60 kHz WWVB and 5 MHz WWV for a path between Ft. Collins, CO and San Antonio, TX were documented. Additionally, deep propagation nulls of WWVB over this path were observed to occur every morning and evening, suggesting

predictable multipath interference between competing daytime and nighttime modes. During the Frequency Measuring Test, propagation-induced frequency variations of 5 MHz WWV were observed at night and especially during dawn and dusk. One observed dawn frequency perturbation was particularly interesting because it occurred at a fundamental frequency shift plus two harmonically related overtones, indicating a nonlinear ionospheric response to rapidly increasing solar radiation.

## August 2017 Eclipse Observations

### Eclipse and Propagation Paths

While much of the USA observed the August 21, 2017 total eclipse through filtered eyeglasses, the station at WA5FRF observed it at LF (60 kHz WWVB) and HF (5 MHz WWV). Figure 1 shows the path of totality and the propagation path between WWVB/WWV for a path between Ft. Collins, CO and San Antonio, TX. The propagation path is completely south of the path of totality, at 153° true, 837 miles, 1348 km, 270 wavelengths at 60 kHz, and 4.5 ms time delay. The



Figure 1 — Paths of totality and propagation.

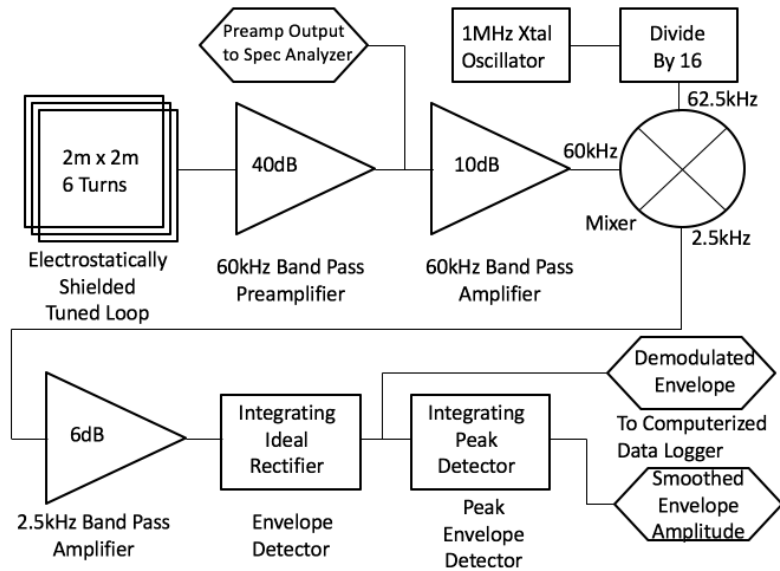


Figure 2 — Superheterodyne receiver used for WWVB.

2 m square formed from PVC pipe. The ends of the cord were interconnected to form a 6-turn coil. Loop area was 4 square meters. Aluminum ducting tape was applied to the outside of the pipe with a narrow gap in the circumference to form an electrostatic shield. The coil was resonated to 60 kHz with approximately 0.02  $\mu\text{F}$  of parallel capacitance and connected to a low-noise preamp made with an LT6231 low noise video op-amp.

The preamp had 40 dB of gain with two outputs. One was for the superheterodyne receiver and another for the spectrum analyzer. Figure 2 shows a block diagram of the receiver.

### Preliminary Waveform Data

An example of the waveforms from the custom WWVB superheterodyne and R9000 receivers are shown in Figure 3. This oscilloscope recording was taken with a time base of 1 second/division to show the structure of the WWVB AM envelope modulation. The bottom trace is the WWVB demodulated envelope voltage; middle trace is the peak WWVB envelope voltage; and the top trace is the R9000 S-meter voltage for 5 MHz WWV. Also evident are the effects of static crashes from lightning. The R9000 derives the S-meter voltage from a fast-attack, slow-decay peak detector circuit operating on the AGC line. A static crash causes a waveform artifact that increases rapidly and decays slowly. The WWVB receiver was specifically designed to suppress this type of artifact in the peak envelope data by using an integrating peak detector with sufficient decay time to faithfully hold the peak amplitude in the face of AM modulation while rolling off the attack time enough to minimize contributions of short static crashes.

For the long-term data records, these three waveforms were digitized by a National Instruments USB-6009 data logger connected to a laptop running NI Signal Express software. The data logger was configured to digitize at a sample rate of 0.035 SPS, or one sample every 28.571 seconds for several reasons. First, sampling at a rate of about twice per minute would give excellent resolution for the anticipated slow changes in propagation caused by the eclipse without producing huge file sizes. However, this rate grossly under samples the data bits of the demodulated WWVB waveform. It was desired to record this waveform in a way that would show both the maximum and minimum waveform amplitudes to monitor both the peak and minimum signal strengths. The receiver noise floor was dominated by atmospheric at the times when the WWVB carrier was completely or nearly completely off. Tracking it along with peak signal amplitude

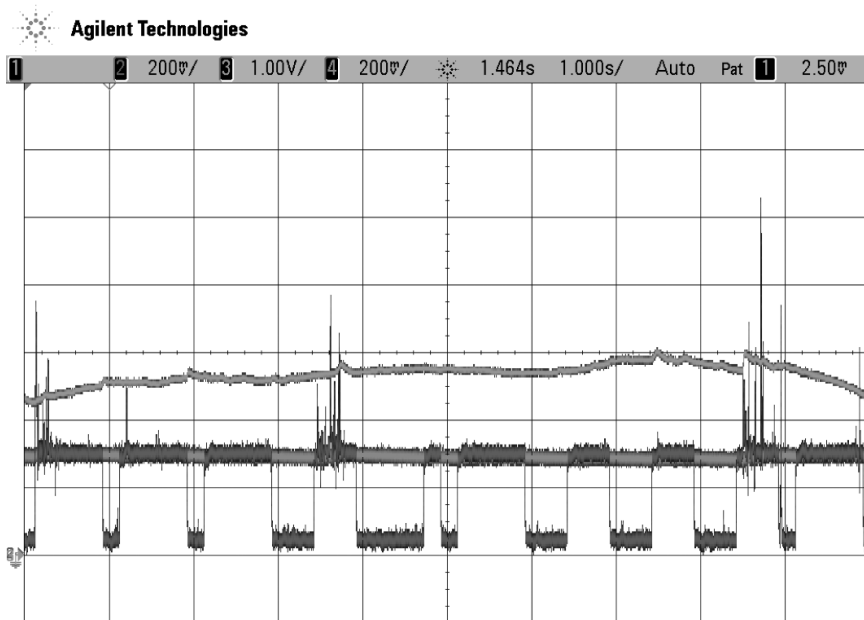


Figure 3 — Expanded scale example of 5 MHz WWV S-meter voltage and WWVB peak and demodulated waveforms sent to data logger.

visible eclipse at WA5FRF was about 70% of totality.

### Instrumentation

The WWV antenna was a horizontal dipole. Receiver was an Icom R9000 with S-meter voltage output. The voltage corresponds to the log of signal strength.

The WWVB antenna was an electrostatically shielded 2 m by 2 m square tuned loop oriented for vertical polarization. The receiver was a custom superheterodyne with

linear envelope and peak-envelope outputs.

Data Logging was automated using the NI USB-6009 digitizer and Signal Express software. Manual observations were with an Anritsu MS2721A spectrum analyzer.

### Custom WWVB Antenna and Receiver

The loop antenna for WWVB was constructed by threading two turns of a piece of 3-conductor extension cord through a 2 m by

could give additional insight to the condition of the ionosphere. A sample rate was required that would sometimes catch the maximum amplitude and sometimes catch the minimum amplitude to produce a “fat” trace whose peak envelope value represented maximum signal strength and whose minimum value was near the ionospheric noise floor. Finally, the sample rate had to be completely asynchronous with the WWVB bit rate to avoid beats in the display that would show up as alternating areas of sparse and dense data. A sample rate of 0.035 SPS worked well. The logging software was set to record 3,024 data samples which gave a record length of 86,400 seconds, or exactly one day.

Figure 4 shows 24-hour data records taken before and after the eclipse on August 10 and 22. The top trace is the R9000 S-meter voltage for 5 MHz WWV. The lower trace is the demodulated WWVB envelope waveform showing both maximum and minimum voltages. The middle trace that rides the top of the lower trace is the WWVB peak envelope voltage. Horizontal scale is time of day beginning on 23:00z the day before. Vertical scale is voltage. The WWVB data is linear in volts, and the WWV data is linear in decibels.

The difference in nighttime vs. daytime propagation is clearly evident for both 5 MHz WWV and 60 kHz WWVB. The transition between nighttime and daytime propagation levels is smooth for WWV but is delineated by local minima for WWVB. Selective fading is observed to be significantly more pronounced at night.

An example of the WWVB spectrum analyzer data is shown in Figure 5. The analyzer was set to average 100 scans to smooth the data. The 10 kHz wide trace shows the shape of the 60 kHz passband set by the high-Q coil resonance and selectivity built into the LNA. Also visible is the spectral peak of WWVB. Two markers were placed on the trace: one at 60 kHz to measure WWVB amplitude, and a second at 61 kHz to record the background noise floor. Both data points were recorded manually at approximately 10 minute intervals during the eclipse and plotted in a spreadsheet. The noise floor varied significantly over the course of a day but better than 10 dB SNR for WWVB was always obtained even during the weakest daytime propagation.

### Measured Propagation Enhancement from the Eclipse

Figure 6 shows the daytime propagation data beginning on the morning of the day of the eclipse. The record begins by showing the propagation of both 5 MHz WWV (upper trace) and WWVB (lower trace) just coming down from night-time levels. The enhancement from the eclipse begins at 16:50z, peaks at 18:04z, and ends at 19:00z. The WWVB enhancement curve is almost triangular, with linear sides and a pointed apex. The WWV data does the same thing but the top of the curve is more rounded due to the linear-in-dB format. The amount of enhancement was about 10 dB for both signals: from  $-90$  to  $-80$  dBm for WWV and from 0.16 to 0.51 V

for WWVB. The amount of enhancement came to within about 10 dB of nighttime levels.

Figure 7 shows the manually taken spectrum analyzer data plotted in a spreadsheet. The horizontal axis is time with Universal Coordinated Time shown at the bottom and Central Daylight Time (local) along the top. The vertical axis is the output of the 40 dB preamp in dBm. Daytime WWVB signal levels are plotted for a day before (19 August, trace truncates at 23:00z), after (22 August, trace truncates at 22:00z), and during the eclipse (21 August, full length trace). The impact of the eclipse is clearly evident and echoes the results obtained with the automated data logger. The measured eclipse-induced enhancement for this measurement was also very close to 10 dB.

### WWVB Morning and Evening Propagation Nulls

The log format of Figure 7 highlights an additional interesting propagation phenomenon. Deep nulls in propagation occurred at local times of 10 a.m. and at 6:30 p.m. Additional lesser nulls occurred during early dawn at 6:30 a.m. and late dusk at 9:45 p.m. These nulls were observed to occur every day. Figure 8A, 8B, and 8C show a collage of data records taken on different days. The transition between nighttime and daytime propagation is not smooth but rather is delineated by these deep propagation nulls in all three plots.

The deep and narrow nature of the nulls

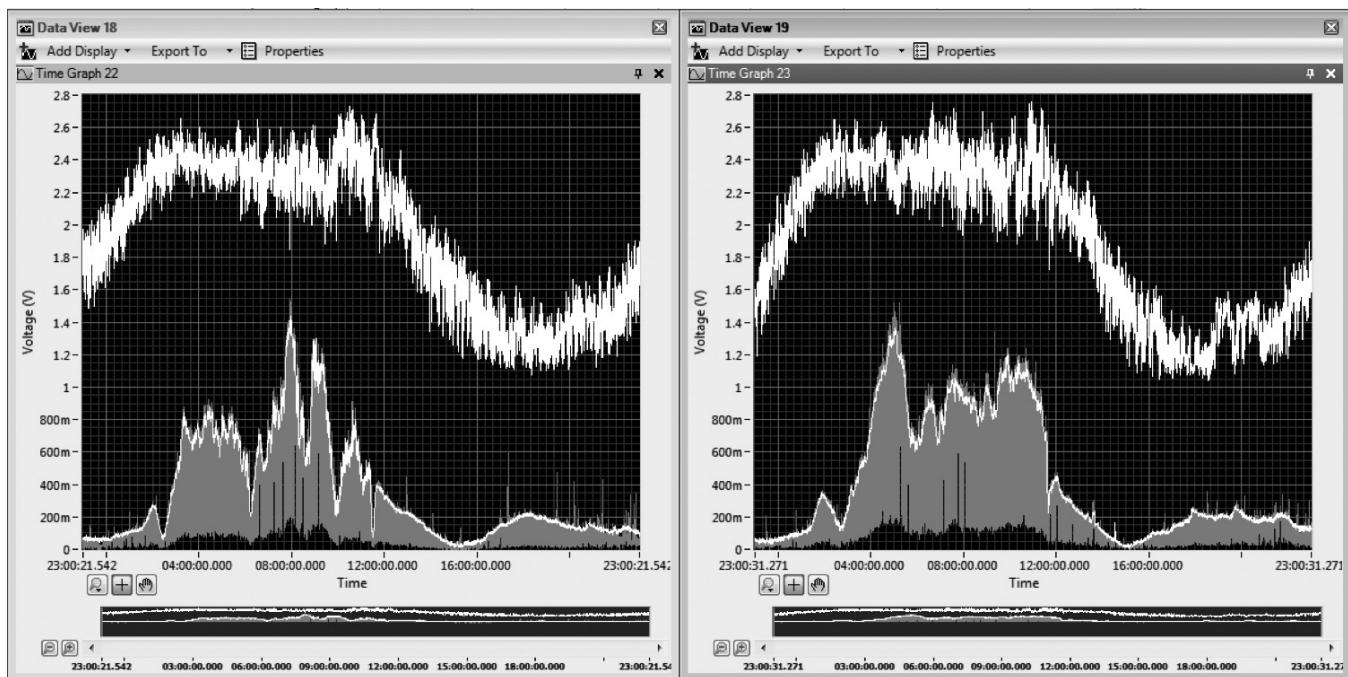


Figure 4 — 24-hour data records taken before and after the eclipse.

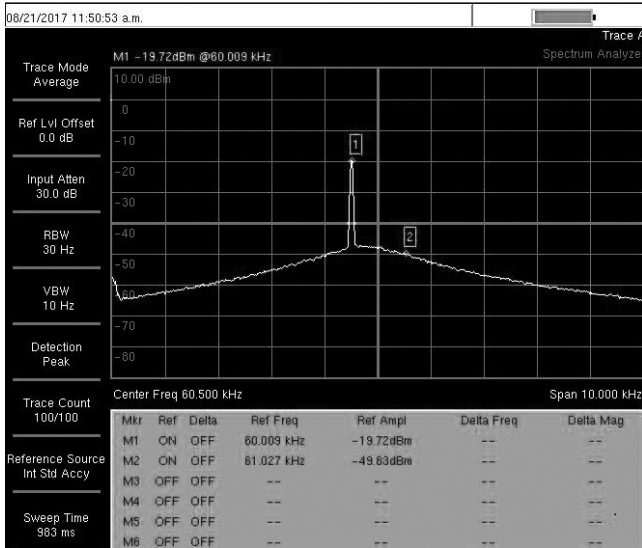


Figure 5 — Example of spectrum analyzer data.

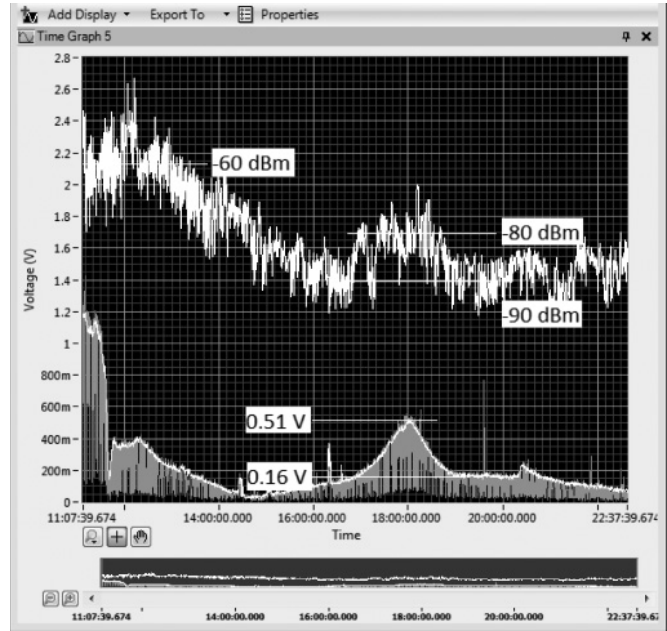


Figure 6 — Eclipse Induced propagation enhancement for 5 MHz WWV and WWVB.

suggests multipath interference between two propagation paths of nearly equal amplitude but opposite phase. Sources of differential phase shift are path length and wave velocity. If nighttime propagation is dominated by ground-hugging ground wave and daytime propagation is via elevated duct, it would not take much elevation change in the elevated duct to create a half-wavelength differential during the time both paths produce comparable signal strengths. The total length of this path is only 270 wavelengths so a half-wave change is less than 0.2%. Another possibility for the phase shift is velocity dispersion in the two paths. The solar radiation changes rapidly in both intensity and angle of incidence during dawn and dusk due to the rotation of the earth. Different ionization levels at different altitudes could create the precise velocity dispersion to cause one path to arrive 180° out of phase with the other. The fact that two nulls were observed every morning and evening suggests the two paths remain open and continue to exhibit phase dispersion over the course of several hours. The less-deep nulls that occur at dawn and dusk indicate that the two paths are 180° out of phase but are of unequal amplitude. But the very deep nulls that occur later in the morning and earlier in the evening indicate that the two paths produce very comparable signal amplitudes. The nulls are absent in the 5 MHz WWV data. Either they do not occur or they did not occur with this setup because the horizontally polarized receive dipole excluded reception of any vertically polarized ground wave component.

The timing of the WWVB major morning and evening nulls was tracked over several days and compared to local sunrise and sunset. Figure 9 graphically depicts the relationship. Timing of the nulls generally tracked sunrise and sunset. As the days got shorter, the morning null occurred later in the day (scatter of points to the right of the ascending sunrise curve) and the evening null occurred earlier (scatter of points to the left of the descending evening curve).

It is interesting that the track of the evening nulls is smooth and very nearly parallels the sunset track. In contrast, the track of the

morning nulls shows significantly more scatter while still generally paralleling the sunrise track. Ionospheric changes seem to happen more violently during the aggressive onset of solar radiation in the morning and decays more gently in the evening as solar radiation wanes and the ionosphere is left to recombine on its own time.

### Propagation Induced Frequency Variations of 5 MHz WWV

Additional interesting propagation effects that affected apparent frequency were

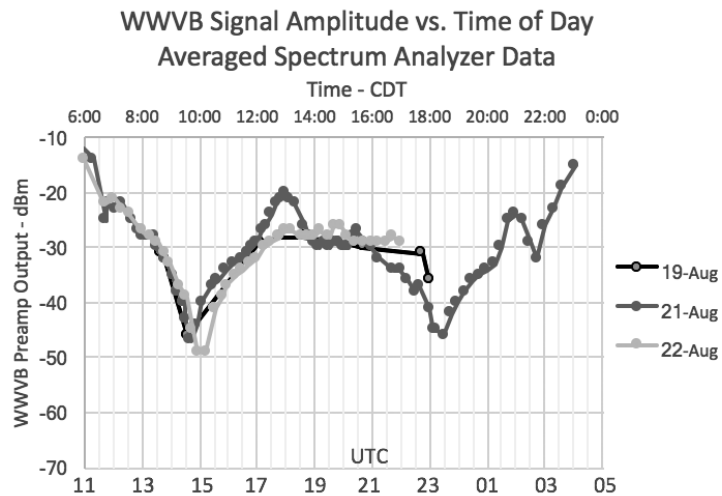
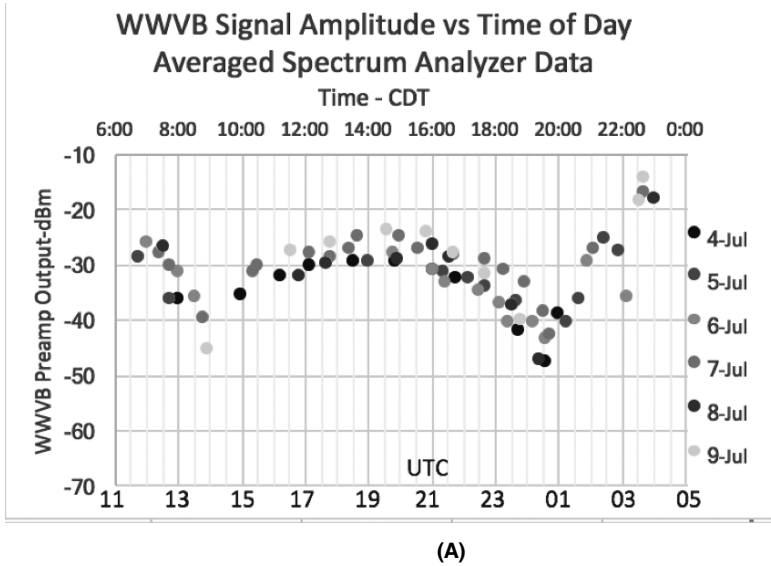
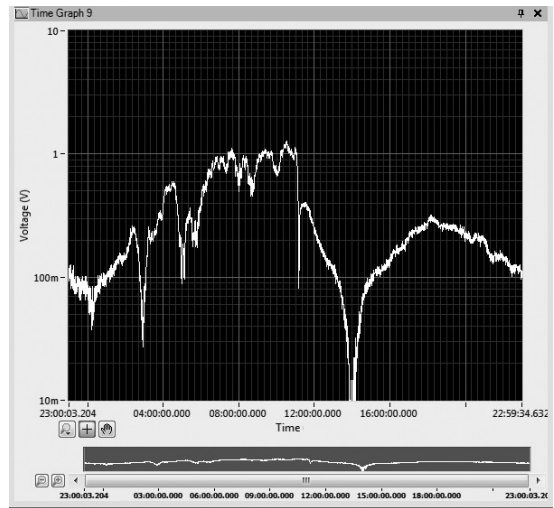


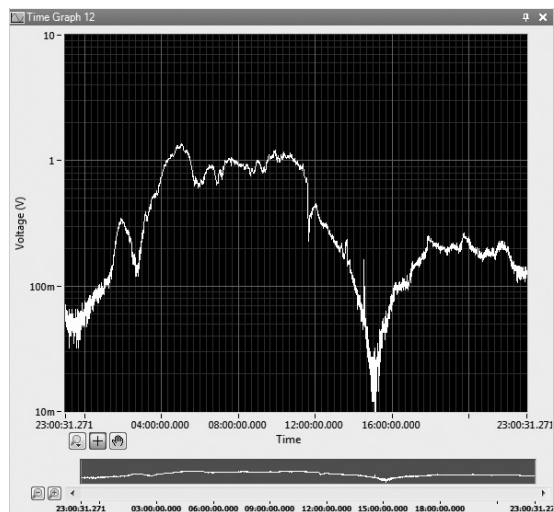
Figure 7 — Manually acquired signal strength from spectrum analyzer.



**Figure 8 — Deep propagation nulls delineate transition between nighttime and daytime propagation every morning and evening.**



(B)



(C)

observed during the ARRL FMT held November 2, 2017. Some of the frequency effects showed similar timing to the signal strength effects described above. During this exercise, GPS-disciplined signals are transmitted on the HF ham bands by a control station, and participants measure the frequency by on-the-air measurements. The signals for the November test were on the 3.5 and 7 MHz Amateur Radio bands. Present state-of-the-amateur-art can accomplish an absolute frequency measurement of sky wave signals at HF to better than 1 Hz and the difference between two proximal frequencies to better than 0.1 Hz. Even the best commercial radio receiver cannot come close to the required accuracy or display precision when used as-is. Calibration to a known source such as the atomic-standard WWV transmission or another GPS-disciplined oscillator is

required. To get the required frequency resolution (several digits to the right of those usually displayed) a common technique is to offset an SSB receiver from the carrier to get an audible beat note and then use an audio spectrum analyzer to get frequency resolution down to several millihertz. While this technique can get you to mHz precision, you cannot get absolute accuracy to that level without taking ionospheric effects into account. Variations in the ionosphere cause apparent frequency shifts that can be on the order of 1 Hz out of 5 MHz. WWV at 5 MHz was chosen as a calibration source because it was between the 3.5 and 7 MHz test frequencies and because the ionospheric paths from the receiver location to both WWV and the FMT transmitter location were in the same direction. The hope was that because of the similar frequencies and propagation paths a

correction factor derived from the 5 MHz WWV would be applicable to 3.5 and 7 MHz. This resulted in the author achieving "Green Box" category in the FMT for absolute accuracy better than 1 Hz and differential accuracy between two tones better than 0.1 Hz for both bands.

The receiver used was an Icom R8600, a modern software defined radio. Some HF receivers use different LO's for different HF bands, so a calibration on one band may not apply to another. Of particular advantage for the R8600 is the fact that it uses a single local oscillator for the entire HF band, so a calibration at 5 MHz would be valid at 3.5 and 7 MHz as well.

Figure 10 shows waterfall displays of the 5 MHz WWV frequency track as seen on the audio spectrum analyzer. Horizontal scale is frequency with a resolution of 0.5 Hz/div

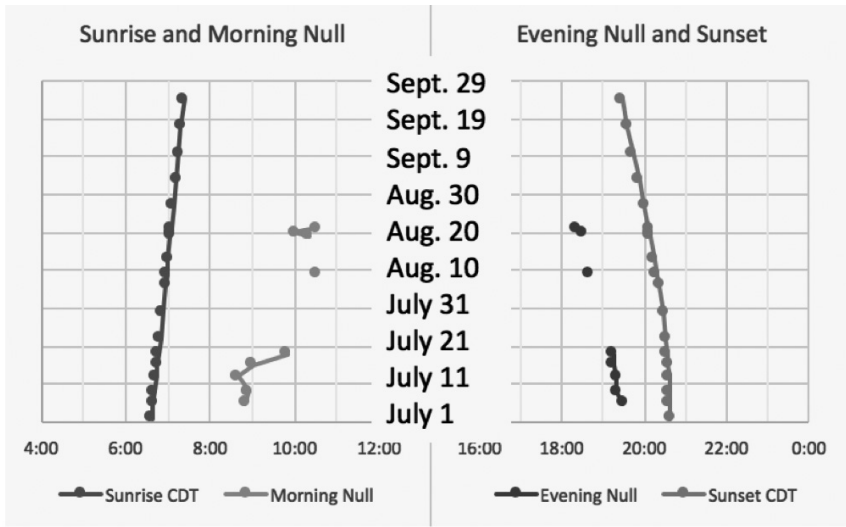


Figure 9 — Timing of morning and evening WWVB nulls were observed to generally track the sun.

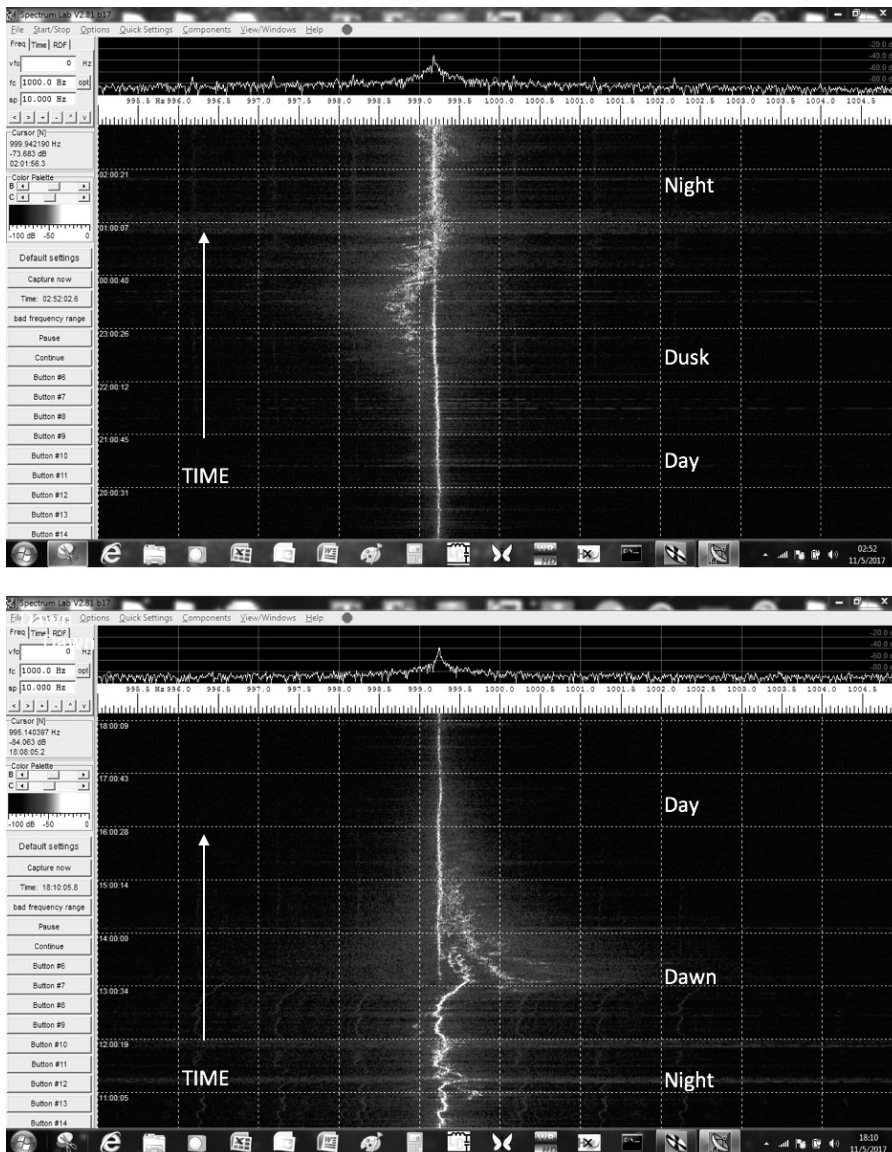


Figure 10 — 5 MHz WWV frequency track during dawn and dusk transitions.

the major divisions and 50 mHz/div for the minor divisions. Receiver dial frequency was set 1 kHz low in USB mode so the 1.000 kHz marker in the center represents an indicated frequency of exactly 5 MHz. Vertical scale is time with each division representing one hour. Older times are at the bottom and newest at the top. Recordings for two 8-hour periods are shown. The bottom recording shows data from night through dawn into day and the top runs from day through dusk back into night. What was interesting was that the apparent frequency of WWV did not remain constant but exhibited diurnal variations with pronounced anti-phased swings at dawn and at dusk.

Apparent frequency variation is quite pronounced at night where significant short term jitter is present. By contrast, daytime propagation is comparatively smooth with smaller and slower undulations. This day/night behavior is similar to the observed WWVB amplitude data that showed significant nighttime selective fading with lesser but smoother propagation anomalies during the day.

The real action in the frequency domain happens at dawn and dusk. Apparent frequency shows a large positive deviation at dawn and a large negative deviation at dusk. Even more interesting is the harmonic overtone structure evident in the dawn data. There is a primary frequency deviation and two successively weaker and harmonically related overtones. Similar to the large scatter in timing of morning propagation nulls, the apparent frequency shift undergoes more radical changes at dawn than at dusk. The rapid onset of solar radiation at dawn evidently drives ionospheric changes more violently than the comparatively gentle recovery period at dusk.

There are at least two possible explanations for the apparent frequency shifts. The shifts have been collectively referred to as “Doppler effects” in the FMT amateur community. Doppler shifts always infer relative motion between source and receiver. They can also occur for fixed transmit and receive locations if a moving reflector is responsible for getting the transmit signal into the receiver (like a police traffic radar). For the apparent frequency deviations to be true Doppler shifts for sky wave signals there must be relative vertical motion in the ionization responsible for propagation between source and receiver. An alternate explanation is simply the large time rate of change in refractive index, or velocity of propagation that occurs during the fast onset and cessation of solar radiation at dawn and dusk. A combination of both effects is possible.

Solar radiation sets free electron density, which in turn sets wave velocity, or index of refraction. For a fixed index, wave speed is a constant fraction of free space velocity and there is no shift in frequency. However, if wave speed is increasing or decreasing, wave front bunching or rarefaction occurs. The net result is identical to closing and receding relative motions with Doppler shifts. Increasing speed is like a source moving towards a receiver and causes an increase in perceived frequency. The opposite holds true for decreasing speed. In Figure 10, the observed positive frequency shift at dawn is indicative of an increasing wave speed as the sun rises. The opposite is true in the evening where the negative frequency shift implies decreasing wave speed. For these effects to be Doppler, respectively descending and ascending ionization in the ionosphere would be required at dawn and dusk. Mathematical analyses on the required velocities for Doppler and index changes for velocity dispersion would give additional insight.

The harmonic overtone structure in the dawn data suggests the presence of nonlinearity. When waves pass through nonlinear media harmonics are generated as well as mixing products if more than one frequency is present. One possibility for the nonlinearity could be a second-derivative effect attributed to the violently changing index caused by the rapid onset of solar radiation at dawn. The index is not only changing, but the rate of change is accelerating. The relationship is similar to that of position, velocity, acceleration, and jerk. Each successive step is the time rate of change, or derivative, of the previous. If you were to graph, for example, position vs. time in the presence of acceleration, the curve would be quite nonlinear. Similarly, an increase in solar flux causes a change in index, and if the rate of change of solar flux is increasing, there is acceleration in wave velocity. Accelerating wave velocity, and perhaps acceleration of the acceleration of wave velocity, could provide the nonlin-

earity responsible for the overtone production in the dawn frequency swing.

---

## Summary

The August 21, 2017 eclipse made a definite and measurable enhancement of LF and HF signals between Ft. Collins, CO and San Antonio, TX. Peak enhancement of 10 dB was measured for both 60 kHz WWVB and 5 MHz WWV signals, coming to within 10 dB of nighttime propagation levels. As expected, 5 MHz WWV exhibited better propagation at night than during the day, with smooth transitions between nighttime and daytime levels.

WWVB also showed better nighttime than daytime propagation but the transitions were delineated by very deep and sharp propagation nulls every morning and evening. The timing of the nulls was observed to track sunrise and sunset from day to day. As the days became shorter the nulls came closer together, occurring later in the morning and earlier in the evening.

The character of the nulls closely resembles the familiar annihilation behavior of the sum of two equal magnitude signals as their phase difference slews through 180°. This suggests the nulls arise from multipath interference between two simultaneous propagation paths that are of comparable amplitude but opposite phase.

WWVB showed significant selective fading at night with many large amplitude swings, sometimes exhibiting pronounced periodicity. By contrast, daytime WWVB propagation exhibited a mostly smooth half-sine wave shape between the morning and evening nulls.

The apparent frequency of 5 MHz WWV showed significant propagation-induced short term jitter at night with smoother, lower frequency undulations during the day. The day/night transitions showed a radical positive frequency swing at dawn and a negative swing at dusk. Additionally, the dawn fre-

quency swing occurred at a fundamental shift plus two harmonically related overtones.

There were interesting correlations between the 60 kHz WWVB amplitude data and the 5 MHz WWV frequency data. During the night, WWVB showed strong selective fading and WWV showed a lot of frequency jitter. During the day, WWVB amplitude and WWV frequency both showed smooth profiles with time. During the day/night transitions, WWVB showed deep amplitude nulls and WWV showed radical frequency swings. In the morning transition, the timing of the WWVB amplitude null smoothly tracked sunset and the WWV frequency swing showed a smooth profile. But in the morning transition, the timing of the WWVB amplitude nulls showed a lot of scatter with relation to sunrise and the WWV frequency swing exhibited harmonic overtones. These correlations highlight the differences between day time and night time propagation and demonstrate how much more aggressively sunrise affects the ionosphere than does sunset.

---

## Acknowledgement

The author would like to thank Bill Liles, NQ6Z, for his many helpful insights and for reviewing this paper.

*Steve Cerwin, WA5FRF, is a physicist with over 40 years experience in designing and building custom instrumentation systems. These systems spanned a range of disciplines including the fields of physics, electronics, acoustic, optics, ionizing radiation, magnetics, and electromagnetics. He spent 38 years at Southwest Research Institute, retiring as an Institute Scientist in 2008. Currently he is still a Technical Advisor for the Institute, operates his own consulting business, and teaches week-long, hands-on antenna courses several times a year. Steve has been a ham radio operator since 1963 and attributes his career in science to an early start in ham radio. He also scuba dives and flies both full scale and RC model aircraft.*